Vol. 34 (2003) ACTA PHYSICA POLONICA B No 5

ABANDONING EXACT SU(3) IN COUPLED-CHANNEL FINAL-STATE INTERACTIONS THROUGH REGGEON EXCHANGE FOR $B \to \pi\pi, K\overline{K}$

P. Łach

H. Niewodniczański Institute of Nuclear Physics
Radzikowskiego 152, 31-342 Kraków, Poland
e-mail: plach@alf.ifj.edu.pl

(Received November 4, 2002)

For weak decays $B_d^0 \to \pi\pi$ and $K\overline{K}$ the effects of SU(3) breaking in coupled-channel final-state interaction effects are discussed in a Regge framework. It is shown that SU(3) breaking in the inelastic final-state transitions dramatically affects the phases of the isospin $I = 0, 1, 2$ amplitudes in the B_d^0 decays. The effect of the singlet penguin diagram on these phases is studied. Furthermore, on the example of the $B_d^0 \to \pi\pi$ decays, the dependence of CP asymmetries on the size of penguin amplitude is analyzed.

PACS numbers: 13.25.Hw, 11.30.Hv, 11.80.Gw, 12.15.Hh

1. Introduction

Final-state interaction (FSI) effects play important role in many physical processes, and in particular in various weak decays. These effects may significantly affect determination of fundamental CP-violating parameters since extraction of the latter requires at least some knowledge of FSI. The role of FSI in B decays was discussed in [1–3]. Unfortunately, understanding it constitutes a difficult task for both theory and phenomenology.

Our model of coupled-channel final-state interaction is based on a quasi-elastic approximation and Regge pole methods [4–6]. The basic physical idea of Regge model is that the high energy behavior of s-channel amplitudes is determined by "exchanges" in the crossed channel. Our model considers rescatterings of the type: $P_iP_j \to P_kP_l$, where P_iP_j and P_kP_l denote pairs of pseudoscalar mesons: $\pi\pi$, $K\overline{K}$, $\eta\eta'$, $\eta\eta$ and $\eta'\eta'$. The dominant exchanges in the t-channel are the Pomeron ($\mathcal{P}$) and the Regge trajectories. In that framework the coupled-channel FSI effects for B_d^0 weak decays into $\pi\pi$ and

$K\overline{K}$ were discussed in Refs. [7]. The calculations [7] were performed under the assumption of the exchange of the ρ, f_2, ω, a_2 Regge trajectories, the trajectories of their SU(3) partners, and the exactly SU(3)-symmetric Pomeron. In this paper we analyze in some details both the influence of SU(3) breaking in the Pomeron, and the influence of singlet penguin amplitude on the predictions of the quasi-elastic coupled-channel Regge approach of Ref. [7]. If SU(3) in the Pomeron is broken and the singlet penguin is not neglected, the conclusions of Refs. [7] would have to be modified.

2. Notation

We use the following phase conventions for pseudoscalar mesons:

$$\begin{aligned}
\pi^+ &= -u\overline{d}\,, \quad \pi^0 = \frac{1}{\sqrt{2}}(u\overline{u} - d\overline{d})\,, \quad \pi^- = d\overline{u}\,,\\
\eta &= \frac{1}{\sqrt{3}}(u\bar{u} + d\bar{d} - s\bar{s})\,, \quad \eta' = \frac{1}{\sqrt{6}}(u\bar{u} + d\bar{d} + 2s\bar{s})\,,\\
K^+ &= u\overline{s}\,, \quad K^0 = d\overline{s}\,, \quad K^- = s\overline{u}\,, \quad \overline{K}^0 = -s\overline{d}\,.
\end{aligned} \tag{1}$$

For Cabibbo-suppressed B_d^0 decays there are nine possible final states composed of two pseudoscalar mesons. In the basis of definite isospin I the symmetrized two-boson states $|(P_kP_l)_I\rangle$ are:

$$\begin{aligned}
|(\pi\pi)_2\rangle &= \frac{1}{\sqrt{6}}(\pi^+\pi^- + \pi^-\pi^+ + 2\pi^0\pi^0),\\
|(K\overline{K})_1\rangle &= \frac{1}{2}(K^+K^- + K^-K^+ + K^0\overline{K^0} + \overline{K^0}K^0),\\
|(\pi^0\eta)_1\rangle &= \frac{1}{\sqrt{2}}(\pi^0\eta + \eta\pi^0),\\
|(\pi^0\eta')_1\rangle &= \frac{1}{\sqrt{2}}(\pi^0\eta' + \eta'\pi^0),\\
|(\pi\pi)_0\rangle &= \frac{1}{\sqrt{3}}(\pi^+\pi^- + \pi^-\pi^+ - \pi^0\pi^0),\\
|(K\overline{K})_0\rangle &= \frac{1}{2}(K^+K^- + K^-K^+ - K^0\overline{K^0} - \overline{K^0}K^0),\\
|(\eta\eta)_0\rangle &= \eta\eta,\\
|(\eta\eta')_0\rangle &= \frac{1}{\sqrt{2}}(\eta\eta' + \eta'\eta),\\
|(\eta'\eta')_0\rangle &= \eta'\eta'.
\end{aligned} \tag{2}$$

3. Quark diagram amplitudes

The decays of B_d^0 mesons to two pseudoscalar mesons ($P_i P_j$) are described by 7 flavor-SU(3) invariant amplitudes [8], but only 4 of them (Fig. 1): "Tree" (T), "Color-suppressed" (C), "Penguin" (P) and additional penguin involving flavor-SU(3)-singlet (S) diagrams, are important [9]. We assume that $|C| = |T|/3|r|$, with $r \approx -3$ [7], $|P| \approx (0.2 \div 0.5)|T|$ [10] and $|S| \approx (0.6 \pm 0.2)|P|$ [10].

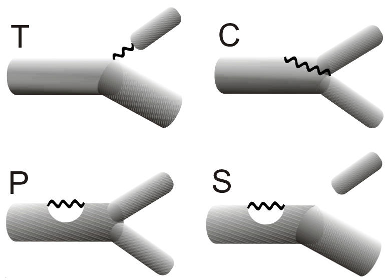

Fig. 1. Graphs describing invariant SU(3)-flavor amplitudes for the decays of B mesons to a pair of light pseudoscalar mesons. (T) "Tree"; (C) "Color-suppressed"; (P) "Penguin"; (S) Additional penguin involving flavor-SU(3)-singlet.

Short-distance amplitudes: T, C, P and S, have weak and strong phases. We can write:

$$\begin{aligned} T &= |T| \mathrm{e}^{i(\gamma+\delta_T)}, \\ C &= |C| \mathrm{e}^{i(\pi+\gamma+\delta_C)}, \text{for } r < 0, \\ P &= |P| \mathrm{e}^{i(-\beta+\delta_P)}, \\ S &= |S| \mathrm{e}^{i(-\beta+\delta_S)}, \end{aligned} \tag{3}$$

where β, γ, (δ) are weak (strong) phases. It is possible that the short-distance weak amplitudes have large strong phases [11]. However, since we want to study FSI we neglect these phases (*i.e.* we set $\delta_T, \delta_C, \delta_P, \delta_S = 0$). For the weak phases we assume [10]

$$\begin{aligned} \gamma &= (60.0^{+5.4}_{-6.8})^\circ \,, \\ \beta &= (22.2 \pm 2.0)^\circ \,. \end{aligned} \tag{4}$$

Furthermore, we neglect the electroweak penguins diagrams [12]. In terms of quark diagram amplitudes the weak decays of B_d^0 to the states defined in Eq. (2) are given by:

$$\langle (\pi\pi)_2 | w | B_d^0 \rangle \; = \; -\frac{1}{\sqrt{6}}(T + C) \,,$$

$$\begin{aligned}
\langle (K\overline{K})_1|w|B_d^0\rangle &= -\frac{1}{2}P\,,\\
\langle (\pi^0\eta)_1|w|B_d^0\rangle &= -\frac{1}{2\sqrt{3}}(2P+S)\,,\\
\langle (\pi^0\eta')_1|w|B_d^0\rangle &= -\frac{1}{\sqrt{6}}(P+2S)\,,\\
\langle (\pi\pi)_0|w|B_d^0\rangle &= -\frac{1}{2\sqrt{3}}(2T-C+3P)\,,\\
\langle (K\overline{K})_0|w|B_d^0\rangle &= \frac{1}{2}P\,,\\
\langle (\eta\eta)_0|w|B_d^0\rangle &= \frac{1}{3}(C+P+S)\,,\\
\langle (\eta\eta')_0|w|B_d^0\rangle &= \frac{1}{6}(2C+2P+5S)\,,\\
\langle (\eta'\eta')_0|w|B_d^0\rangle &= \frac{1}{6}(C+P+4S)\,. \qquad (5)
\end{aligned}$$

We assumed SU(3) symmetry in weak decays, *i.e.* equal amplitudes for the production of strange ($s\overline{s}$) and nonstrange quark pairs.

4. Final state interaction

4.1. General framework

The weak amplitude w is changed by isospin-conserving strong interaction S_{FSI} in the final state [7] into a FSI-corrected weak amplitude W:

$$(B_d^0 \xrightarrow{w} (P_iP_j)_I \xrightarrow{S_{\mathrm{FSI}}} (P_kP_l)_I) \equiv B_d^0 \xRightarrow{W} (P_kP_l)_I\,, \qquad (6)$$

where subscript I denotes isospin. We describe S_{FSI} in the Regge pole model as used in [4–7]. In the energy range $s \simeq {m_{B_d}}^2 = 27.88$ GeV^2 the Pomeron ($\mathcal{P}$) contribution to the t-channel amplitude is phenomenologically well described by the formula [6]

$$A_{\mathcal{P}}(P_iP_j) = i\beta_{\mathcal{P}}^{P_i}\beta_{\mathcal{P}}^{P_j}\,\mathrm{e}^{i(b_{\mathcal{P}}^{P_i}+b_{\mathcal{P}}^{P_j})t}s\,, \qquad (7)$$

where the residue $\beta_{\mathcal{P}}^{P_i}\beta_{\mathcal{P}}^{P_j}$ and slope $b_{\mathcal{P}}^{P_i}+b_{\mathcal{P}}^{P_j}$ depend on the scattering process considered. Calculations of the s-channel $l=0$ waves $a_{\mathcal{P}}(P_iP_j)$, give, for the Pomeron [6]:

$$a_{\mathcal{P}}(P_iP_j) = i\mathcal{P}_{P_iP_j} = i\frac{\beta_{\mathcal{P}}^{P_i}\beta_{\mathcal{P}}^{P_j}}{b_{\mathcal{P}}^{P_i}+b_{\mathcal{P}}^{P_i}}\,. \qquad (8)$$

From [14,15] we obtain

$$\beta^{\pi}_{\mathcal{P}} = 3.48\sqrt{\mathrm{mb}}\,, \tag{9}$$
$$\beta^{K}_{\mathcal{P}} = 2.74\sqrt{\mathrm{mb}} \tag{10}$$

and

$$b^{\pi}_{\mathcal{P}} = 2.06\mathrm{GeV}^{-2}\,, \tag{11}$$
$$b^{K}_{\mathcal{P}} = 0.8\mathrm{GeV}^{-2}\,. \tag{12}$$

The simple relations between $\beta^{\eta(\eta')}_{\mathcal{P}}$, $b^{\eta(\eta')}_{\mathcal{P}}$ and $\beta^{\pi(K)}_{\mathcal{P}}$, $b^{\pi(K)}_{\mathcal{P}}$ for broken SU(3) are given by

$$\beta^{\eta}_{\mathcal{P}} = \frac{1}{3}(\beta^{\pi}_{\mathcal{P}} + 2\beta^{K}_{\mathcal{P}})\,, \tag{13}$$
$$\beta^{\eta'}_{\mathcal{P}} = \frac{1}{3}(-\beta^{\pi}_{\mathcal{P}} + 4\beta^{K}_{\mathcal{P}})\,, \tag{14}$$

and

$$b^{\eta}_{\mathcal{P}} = \frac{1}{3}(b^{\pi}_{\mathcal{P}} + 2b^{K}_{\mathcal{P}})\,, \tag{15}$$
$$b^{\eta'}_{\mathcal{P}} = \frac{1}{3}(-b^{\pi}_{\mathcal{P}} + 4b^{K}_{\mathcal{P}})\,. \tag{16}$$

From Eqs. (8)–(16) we find:

$$\begin{aligned}
\mathcal{P}_{\pi\pi} &= 2.9\ \ \mathrm{mb\,GeV}^2\,,\\
\mathcal{P}_{K\overline{K}} &= 4.9\ \ \mathrm{mb\,GeV}^2\,,\\
\mathcal{P}_{\pi\eta} &= 3.2\ \ \mathrm{mb\,GeV}^2\,,\\
\mathcal{P}_{\pi\eta'} &= 3.6\ \ \mathrm{mb\,GeV}^2\,,\\
\mathcal{P}_{\eta\eta} &= 3.7\ \ \mathrm{mb\,GeV}^2\,,\\
\mathcal{P}_{\eta'\eta} &= 4.8\ \ \mathrm{mb\,GeV}^2\,,\\
\mathcal{P}_{\eta'\eta'} &= 8.7\ \ \mathrm{mb\,GeV}^2\,.
\end{aligned} \tag{17}$$

In the SU(3) symmetric case we have $\mathcal{P}_{P_iP_j} = \mathcal{P} = 3.6$ mb GeV^2.

Many authors restrict their studies to elastic rescattering only. In Regge language this is described in terms of a Pomeron exchange. But at $s = m_B^2$ contributions from other inelastic nonleading Regge exchanges are not completely negligible [7]. There are two types of contributions from exchange-degenerate Reggeons corresponding to two different diagrams (crossed $\boldsymbol{C}$ and uncrossed $\boldsymbol{U}$, see Fig. 2). The contributions of diagrams $\boldsymbol{U}$ and $\boldsymbol{C}$ differ

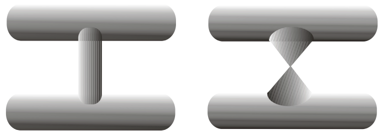

Fig. 2. FSI diagrams ($\boldsymbol{U}$) Uncrossed Reggeon exchange, ($\boldsymbol{C}$) Crossed Reggeon exchange.

in their phases [7]. The calculations of the s-channel $l = 0$ partial waves amplitudes a_U for uncrossed Reggeon exchange and a_C for crossed Reggeon exchange give [6]:

$$a_U = -\frac{R}{\alpha'} \frac{i(\frac{s}{s_0})^{-1/2}(\ln\frac{s}{s_0} + i\pi)}{\ln^2\frac{s}{s_0} + \pi^2} \tag{18}$$

and

$$a_C = \frac{R}{\alpha'} \frac{(\frac{s}{s_0})^{-1/2}}{\ln\frac{s}{s_0}}\,, \tag{19}$$

where R is the Regge residue fitted from experiment [7, 15] :

$$R = -4g^2(\omega, KK) = -\frac{4}{9}g^2(\omega, pp) = -13.1 \text{ mb}, \tag{20}$$

and

$$\alpha' \approx 1 \text{ GeV}^{-2}. \tag{21}$$

The scale factor s_0 is taken as 1GeV^2.

Inelastic FSI means here the coupled-channel effects of the type: $\pi\pi \to K\overline{K}$, $\eta_8\eta_8$, $\eta_1\eta_8$, $\ldots$, and $K\overline{K} \to \pi\pi$, $\eta_8\eta_8$, $\eta_1\eta_8$, $\ldots$etc in the final state. Inclusion of such processes was shown in [7] to be very important. There are three separate non-communicating FSI sectors of different isospin ($I = 0, 1, 2$).

In the $I = 2$ sector one obtains only the contribution from the crossed diagram of Fig. 2:

$$\boldsymbol{U}_2 = [\langle(\pi\pi)_2|\boldsymbol{U}_2|(\pi\pi)_2\rangle] = 0\,, \tag{22}$$

$$\boldsymbol{C}_2 = [\langle(\pi\pi)_2|\boldsymbol{C}_2|(\pi\pi)_2\rangle] = 2\,. \tag{23}$$

In the $I = 1$ sector there are three states, and consequently we have coupled-channel effects described together with quasi-elastic effects by two 2×2 matrices. One obtains:

$$\boldsymbol{U}_1 = [\langle i|\boldsymbol{U}_1|j\rangle] = \begin{bmatrix} \varepsilon^2 & \frac{2}{\sqrt{3}}\varepsilon & \sqrt{\frac{2}{3}}\varepsilon \\ \frac{2}{\sqrt{3}}\varepsilon & \frac{4}{3} & \frac{2}{3}\sqrt{2} \\ \sqrt{\frac{2}{3}}\varepsilon & \frac{2}{3}\sqrt{2} & \frac{2}{3} \end{bmatrix} \tag{24}$$

and

$$\boldsymbol{C}_1 = [\langle i|\boldsymbol{C}_1|j\rangle] = \begin{bmatrix} 0 & -\frac{2}{\sqrt{3}}|\varepsilon| & 2\sqrt{\frac{2}{3}}|\varepsilon| \\ -\frac{2}{\sqrt{3}}|\varepsilon| & \frac{4}{3} & \frac{2}{3}\sqrt{2} \\ 2\sqrt{\frac{2}{3}}|\varepsilon| & \frac{2}{3}\sqrt{2} & \frac{2}{3} \end{bmatrix}. \tag{25}$$

The states in the rows and columns are (from top to bottom and from left to right): $i,j = |(K\overline{K})_1\rangle$, $|(\pi^0\eta)_1\rangle$ and $|(\pi^0\eta')_1\rangle$.

In the $I = 0$ sector there are five states with rows and columns corresponding to the states (from top to bottom and from left to right): $i,j = |(\pi\pi)_0\rangle$, $|(K\overline{K})_0\rangle$, $|(\eta\eta)_0\rangle$, $|(\eta\eta')_0\rangle$ and $|(\eta'\eta')_0\rangle$. One obtains:

$$\begin{aligned} \boldsymbol{U}_0 &= [\langle i|\boldsymbol{U}_0|j\rangle] \\ &= \begin{bmatrix} 3 & -\sqrt{3}\varepsilon & -\frac{2}{\sqrt{3}} & -\frac{2}{\sqrt{3}} & -\frac{1}{\sqrt{3}} \\ -\sqrt{3}\varepsilon & \varepsilon^2+2 & \frac{4}{3}\varepsilon & -\frac{2}{3}\varepsilon & \frac{5}{3}\varepsilon \\ -\frac{2}{\sqrt{3}} & \frac{4}{3}\varepsilon & \frac{2}{9}(2+\varepsilon^2) & \frac{4}{9}(1-\varepsilon^2) & \frac{2}{9}(1+2\varepsilon^2) \\ -\frac{2}{\sqrt{3}} & -\frac{2}{3}\varepsilon & \frac{4}{9}(1-\varepsilon^2) & \frac{4}{9}(1+2\varepsilon^2) & \frac{2}{9}(1-4\varepsilon^2) \\ -\frac{1}{\sqrt{3}} & \frac{5}{3}\varepsilon & \frac{2}{9}(1+2\varepsilon^2) & \frac{2}{9}(1-4\varepsilon^2) & \frac{1}{9}(1+8\varepsilon^2) \end{bmatrix} \end{aligned} \tag{26}$$

and

$$\begin{aligned} \boldsymbol{C}_0 &= [\langle i|\boldsymbol{C}_0|j\rangle] \\ &= \begin{bmatrix} -1 & 0 & -\frac{2}{\sqrt{3}} & -\frac{2}{\sqrt{3}} & -\frac{1}{\sqrt{3}} \\ 0 & 0 & -\frac{4}{3}|\varepsilon| & \frac{2}{3}|\varepsilon| & \frac{4}{3}|\varepsilon| \\ -\frac{2}{\sqrt{3}} & -\frac{4}{3}|\varepsilon| & \frac{2}{9}(2+1|\varepsilon|^2) & \frac{4}{9}(1-|\varepsilon|^2) & \frac{2}{9}(1+2|\varepsilon|^2) \\ -\frac{2}{\sqrt{3}} & \frac{2}{3}|\varepsilon| & \frac{4}{9}(1-|\varepsilon|^2) & \frac{4}{9}(1+2|\varepsilon|^2) & \frac{2}{9}(1-4|\varepsilon|^2) \\ -\frac{1}{\sqrt{3}} & \frac{4}{3}|\varepsilon| & \frac{2}{9}(1+2|\varepsilon|^2) & \frac{2}{9}(1-4|\varepsilon|^2) & \frac{1}{9}(1+8|\varepsilon|^2) \end{bmatrix}. \end{aligned} \tag{27}$$

The parameter ε (ε^2) describes suppression of propagation of one (two) strange quarks in the t-channel. For the SU(3) discussion of coupled-channel effects $\varepsilon = 1$ [7]. A more realistic assumption used in this paper is:

$$\varepsilon = (-\frac{s}{s_0})^{\alpha_0(K^*)-\alpha_0(\rho)} \approx 0.5\mathrm{e}^{-i36^\circ}, \tag{28}$$

where $\alpha_0(K^*) \approx 0.3$ and $\alpha_0(\rho) \approx 0.5$ are Reggeon's parameters.

Let us now connect weak decays and strong interactions in the final state. We can obtain amplitudes $\langle (P_iP_j), I|W|B_d^0\rangle$ of B_d^0 decay to states $(P_iP_j)_I$ from:

$$\begin{aligned} &\langle (P_iP_j), I|W|B_d^0\rangle = \langle (P_iP_j), I|S_{\mathrm{FSI}}^{1/2} w|B_d^0\rangle \\ &= \sum_{\boldsymbol{V}} \langle (P_iP_j), I|\boldsymbol{V}, I\rangle\langle \boldsymbol{V}, I|S_{\mathrm{FSI}}^{1/2}|\boldsymbol{V}, I\rangle\langle (P_iP_j), I|w|B_d^0\rangle\,, \end{aligned} \tag{29}$$

with $\langle (P_iP_j), I|\boldsymbol{V}, I\rangle$ are eigenvectors for $S^{1/2}_{\rm FSI}(I) = iP + a_U U_I + a_C C_I$ matrices. We assume now that the FSI-corrected weak decay amplitudes differ from quark-level expressions (Eq. (5)) by hadronic phase factors only ($S_{\rm FSI} = {\rm e}^{2i\delta}$) [6, 7].

4.2. Numerical results

Using Eq. (29) one obtains the numbers given in the right-hand side of Tables I, II and in Table III. For the sake of comparison, in the left-hand side of Tables I, II we added amplitude phases with SU(3) symmetric FSI (Table I), as well as amplitude phases calculated without FSI effects (Table II). In order to make comparison with [7] possible, we first put the

TABLE I

Comparison of calculated values of amplitude phases for B^0_d decays with weak phases set to 0.

Phase φ, $\varphi \in (-180^\circ, 180^\circ)$	No c. c.	Coupled channels (c. c.)							
	$\varepsilon = 1$					$\varepsilon = 0.5{\rm e}^{-i36^\circ}$			
	Ref. [7], $\mathcal{P} = 3.6$mbGeV^2			SU(3)broken in Pomerons				$\mathcal{P} =$ 3.6 mbGeV^2	
		$\lvert P\rvert/\lvert T\rvert =$ 0.04	0.2	0.04	0.2	0.04	0.2	0.04	0.2
$\varphi^2_{\pi\pi}$	112°	112°	112°	117°	117°	117°	117°	112°	112°
$\varphi^0_{\pi\pi}$	94°	93°	94°	85°	89°	89°	91°	92°	94°
$\varphi^2_{\pi\pi} - \varphi^0_{\pi\pi}$	18°	19°	18°	32°	28°	28°	26°	20°	18°
$\varphi^1_{K\bar{K}}$	95°	85°	85°	104°	103°	91°	91°	93°	93°
$\varphi^0_{K\bar{K}}$	103°	168°	137°	168°	123°	110°	98°	123°	113°
$\varphi^1_{K\overline{K}} - \varphi^0_{K\overline{K}}$	−8°	−83°	−52°	−59°	−20°	−19°	−7°	−30°	−20°

phases β and γ to zero. For this case, in Table I we present the dependence of amplitude phases on SU(3) breaking in the Pomeron coupling ($\mathcal{P}_{P_iPj}$) and through the parameter ε, and on the combination of these two effects. It is interesting to see where SU(3) breaking is important for numerical results. If we switch SU(3) breaking on in Pomerons only, and compare with [7] (left-hand side of Table I) we obtain for $|P|/|T| = 0.2$: $\varphi^2_{\pi\pi} - \varphi^0_{\pi\pi} = 18^\circ \to 28^\circ$ and $\varphi^1_{K\overline{K}} - \varphi^0_{K\overline{K}} = -52^\circ \to -20^\circ$. The effect is large. If we switch SU(3) breaking on only in ε ($\mathcal{P}_{P_iPj} = 3.6$ mbGeV^2), we obtain: $\varphi^2_{\pi\pi} - \varphi^0_{\pi\pi} = 18^\circ \to 18^\circ$ and $\varphi^1_{K\overline{K}} - \varphi^0_{K\overline{K}} = -52^\circ \to -20^\circ$. We see that in this case we may neglect the effect of SU(3) breaking in $(\pi\pi)_I$ phases, but in $(K\overline{K})_I$ phases the effect is large. Now, we combine both effects. Comparing appropriate columns we see that: $\varphi^2_{\pi\pi} - \varphi^0_{\pi\pi} = 18^\circ \to 26^\circ$ and $\varphi^1_{K\overline{K}} - \varphi^0_{K\overline{K}} = -52^\circ \to -7^\circ$ for $|P|/|T| = 0.2$. We see that in $(K\overline{K})_I$ both effects are important, and neither of them can be neglected.

TABLE II

Comparison of calculated values of phase shifts for B_d^0 decays in case of nonzero weak phases.

Phase φ, $\varphi \in (-180°, 180°)$	No FSI			Coupled channels with SU(3) breaking					
	$S=0$						$\|S\|/\|P\|=0.6$		
	$\|P\|/\|T\|=$								
	0.04	0.2	0.35	0.04	0.2	0.35	0.2	0.35	0.5
$\varphi^2_{\pi\pi}$	$-120°$	$-120°$	$-120°$	$-3°$	$-3°$	$-3°$	$-3°$	$-3°$	$-3°$
$\varphi^0_{\pi\pi}$	$-123°$	$-135°$	$-145°$	$-39°$	$-49°$	$-56°$	$-47°$	$-53°$	$-58°$
$\varphi^2_{\pi\pi}-\varphi^0_{\pi\pi}$	$3°$	$15°$	$25°$	$36°$	$46°$	$53°$	$44°$	$50°$	$55°$
$\varphi^1_{K\bar{K}}$	$158°$	$158°$	$158°$	$-98°$	$-98°$	$-98°$	$-84°$	$-84°$	$-84°$
$\varphi^0_{K\bar{K}}$	$-22°$	$-22°$	$-22°$	$104°$	$81°$	$80°$	$94°$	$91°$	$90°$
$\varphi^1_{K\overline{K}}-\varphi^0_{K\overline{K}}$	$180°$	$180°$	$180°$	$158°$	$179°$	$178°$	$-178°$	$-175°$	$-174°$

The numbers given in Table II are obtained with realistic weak phases of Eq. (4). Comparing appropriate columns in Table II we see that inclusion of weak phases and coupled-channel effects change amplitude phases in the considered model: $\varphi^2_{\pi\pi}-\varphi^0_{\pi\pi}=25° \to 53°$ and $\varphi^1_{K\overline{K}}-\varphi^0_{K\overline{K}}=180° \to 178°$ for $|P|/|T|=0.35$. Amplitude phases strongly depend on the ratio $|P|/|T|$, for instance: $\varphi^0_{K\overline{K}}(|P|/|T|=0.35, S=0)-\varphi^0_{K\overline{K}}(|P|/|T|=0.04, S=0)=-24°$. However in the region $|P|/|T| \in (0.2, 0.5)$ the dependence is not strong (no more than 7°).

TABLE III

Influence of the singlet penguin on phase shifts in B_d^0 decays.

Phase φ, $\varphi \in (-180°, 180°)$	$S=0$			$\|S\|=0.6\|P\|$		
	$\|P\|/\|T\|=$					
	0.2	0.35	0.5	0.2	0.35	0.5
$\varphi^1_{\pi^0\eta}$	$-95°$	$-95°$	$-95°$	$-82°$	$-90°$	$-90°$
$\varphi^1_{\pi^0\eta'}$	$-70°$	$-70°$	$-70°$	$-86°$	$-86°$	$-86°$
$\varphi^0_{\eta\eta}$	$-127°$	$-160°$	$157°$	$-140°$	$136°$	$109°$
$\varphi^0_{\eta\eta'}$	$-133°$	$-179°$	$148°$	$140°$	$105°$	$100°$
$\varphi^0_{\eta'\eta'}$	$160°$	$115°$	$114°$	$74°$	$79°$	$81°$

Now we discuss the influence of the singlet penguin. From Table II we see that the phases for decays $B_d^0 \to \pi\pi, K\overline{K}$ do not depend very strongly on the inclusion of the singlet penguin, for instance: $\varphi^0_{\pi\pi}(|P|/|T|=0.35, |S|/|P|=0.6)-\varphi^0_{\pi\pi}(|P|/|T|=0.35, S=0)=-3°$, $\varphi^0_{K\overline{K}}(|P|/|T|=0.35, |S|/|P|=0.6)-\varphi^0_{K\overline{K}}(|P|/|T|=0.35, S=0)=11°$. Thus, for $B_d^0 \to \pi\pi, K\overline{K}$ the effect of the singlet penguin may be neglected. However, from Table III we see that the influence of the singlet penguin for decays $B_d^0 \to \eta\eta, \eta\eta', \eta'\eta'$ is very large: $\varphi^0_{\eta\eta}(|P|/|T| = 0.35, |S|/|P| = 0.6) - \varphi^0_{\eta\eta}(|P|/|T| = 0.35, S = 0) = -64^\circ(+360^\circ)$, $\varphi^0_{\eta\eta'}(|P|/|T| = 0.35, |S|/|P| = 0.6) - \varphi^0_{\eta\eta'}(|P|/|T| = 0.35, S = 0) = -76^\circ(+360^\circ)$, $\varphi_{\eta'\eta'}(|P|/|T| = 0.35, |S|/|P| = 0.6) - \varphi_{\eta'\eta'}(|P|/|T| = 0.35, S = 0) = 35^\circ$. The singlet penguin is very important for channels which contain the η and η' mesons.

5. CP violation

It is interesting to calculate the CP-violation effects in our model. CP-violating asymmetries for the decays of a neutral B_d into final states $\pi^+\pi^-$ and $\pi^0\pi^0$ are defined as

$$\mathcal{A}_{\pi^+\pi^-} = \frac{|\langle\pi^+\pi^-|W|\overline{B}{}^0_d\rangle|^2 - |\langle\pi^+\pi^-|W|B^0_d\rangle|^2}{|\langle\pi^+\pi^-|W|\overline{B}{}^0_d\rangle|^2 + |\langle\pi^+\pi^-|W|B^0_d\rangle|^2} \tag{30}$$

and

$$\mathcal{A}_{\pi^0\pi^0} = \frac{|\langle\pi^0\pi^0|W|\overline{B}{}^0_d\rangle|^2 - |\langle\pi^0\pi^0|W|B^0_d\rangle|^2}{|\langle\pi^0\pi^0|W|\overline{B}{}^0_d\rangle|^2 + |\langle\pi^0\pi^0|W|B^0_d\rangle|^2}\,, \tag{31}$$

with

$$\langle\pi^+\pi^-|W|B^0_d\rangle = \sqrt{\frac{2}{3}}\langle(\pi\pi)_0|W|B^0_d\rangle + \frac{1}{\sqrt{3}}\langle(\pi\pi)_2|W|B^0_d\rangle\,, \tag{32}$$

$$\langle\pi^0\pi^0|W|B^0_d\rangle = -\frac{1}{\sqrt{3}}\langle(\pi\pi)_0|W|B^0_d\rangle + \sqrt{\frac{2}{3}}\langle(\pi\pi)_2|W|B^0_d\rangle\,. \tag{33}$$

CP violation is still one of the least tested aspects of the Standard Model. Current data exhibit CP violation in the B_d sector with large errors [16–18]. In Fig. 3 we show the dependence of CP asymmetry on the size of penguin contribution. For small $\mathcal{A}_{\pi\pi}$ the ratio $|P|/|T|$ should be very small. CP violation effects are more pronounced in the $\pi^0\pi^0$ channel, for example for $|P|/|T| = 0.35$ we have $\mathcal{A}_{\pi^+\pi^-} = -0.19$, and $\mathcal{A}_{\pi^0\pi^0} = -0.99$. Large values of these CP asymmetries were obtained in other papers as well [20, 21]. In our case, for $|P|$ comparable to $|T|$ the large size of predicted CP asymmetry is permitted by fairly large FSI-induced phase shifts.

CP asymmetries depend on strong phases ($\delta_T, \delta_C, \delta_P$, and δ_S) of short-distance amplitudes (3). We know nothing about the size of these parameters. In [19] it is shown that for the current data these phases may be in the region $(-90^\circ, 90^\circ)$ [16–18]. In order to show how these phases may affect the calculations a few arbitrary phases where chosen. The results are given

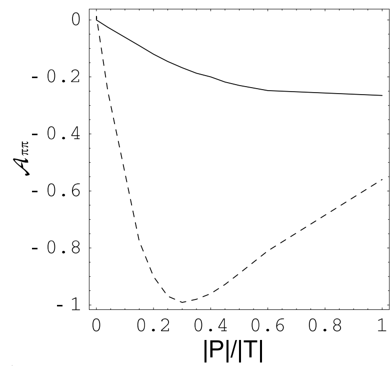

Fig. 3. Influence of penguin contribution on CP asymmetry in decays $B_d^0 \to \pi^+\pi^-$ (solid line), and $B_d^0 \to \pi^0\pi^0$ (dashed line).

in Table IV. We assume that $\delta_T = \delta_C = \delta_{TC}$ and $\delta_P = \delta_S = \delta_{PS}$. From Table IV we see that CP asymmetries (for $|P|/|T| = 0.35$) depend very strongly on these phases, for example: $\mathcal{A}_{\pi^0\pi^0} \approx -1$ when we neglect short-distance amplitude phases, but $\mathcal{A}_{\pi^0\pi^0} = -0.58$ for $\delta_{TC} = 30°$ and $\delta_{PS} = -20°$. As shown in Table IV the CP asymmetries do not depend significantly on ε (Eq. (28)), so we may keep SU(3) symmetry in matrices $\boldsymbol{U}$ and $\boldsymbol{C}$ when analyzing CP violation. The origin of big CP asymmetry lies in the joint effect of weak phases γ and β and strong phases from inelastic rescattering, and short distance amplitudes. Effects from FSI and short-distance amplitude mix. Both effects give important contributions to CP asymmetry.

TABLE IV

Influence of strong phases δ_{TC} and δ_{PS} of T, C, P, and S amplitudes on CP asymmetries in decays $B_d^0 \to \pi\pi$, for $|P|/|T| = 0.35$.

$\mathcal{A}_{\pi\pi}$	ε Eq. (28)	Strong phases δ_{TC}, δ_{PS} = $0°, 0°$	$30°, -20°$	$-20°, 30°$
$\mathcal{A}_{\pi^+\pi^-}$	$0.5e^{-i36°}$	−0.19	0.33	−0.60
	1	−0.19	0.30	−0.57
$\mathcal{A}_{\pi^0\pi^0}$	$0.5e^{-i36°}$	−0.99	−0.58	−0.70
	1	−1	−0.63	−0.65

One has to realize, that for $l = 0$ partial wave amplitudes the Regge pole methods need not be reliable [12] and, consequently, the obtained numbers should be considered as rough estimates only. In addition to FSI effects and hadronic phases of 'bare' weak diagrams, CP violation effects may strongly depend on electroweak diagrams [12], but there is not enough data to determine the corresponding parameters.

6. Conclusions

In summary, we have discussed the effect of abandoning exact SU(3) in coupled-channel final-state interactions through Reggeon exchange for $B_d^0 \to \pi\pi, K\overline{K}$. SU(3) was broken by admitting lower lying trajectories for strange Reggeons $|\varepsilon| < 1$ (Eq. (28)) and in the Pomeron (Eq. (17)) couplings. As expected in [7] the singlet penguin diagram may be neglected in intermediate states of $B_d^0 \to \pi\pi, K\overline{K}$ decays. However, it cannot be neglected in decays to $\eta\eta$, $\eta\eta'$, and $\eta'\eta'$. We have shown that strong FSI play an important role in the analysis of CP-violating effects in B decays. The size of CP asymmetry in $B_d^0 \to \pi\pi$ decays has been shown to depend strongly on the ratio of penguin to tree amplitude and on the strong phases of short-distance quark diagrams.

I would like to thank P. Żenczykowski for discussions and comments regarding the presentation of the material of this paper.

REFERENCES

[1] P. Żenczykowski, *Acta Phys. Pol. B* **28**, 1605 (1997).
[2] J.F. Donoghue *et al.*, *Phys. Rev.* **D33**, 1516 (1986).
[3] L. Wolfenstein, *Phys. Rev.* **D52**, 537 (1995).
[4] J.-M. Gérard, J. Weyers, *Eur. Phys. J.* **C7**, 1 (1999).
[5] D. Delépine, J.-M. Gérard, J. Pestieau, J. Weyers, *Phys. Lett.* **B429**, 106 (1998).
[6] J.-M. Gérard, J. Pestieau, J. Weyers, *Phys. Lett.* **B436**, 363 (1998).
[7] P. Żenczykowski, *Phys. Lett.* **B460**, 390 (1999).
[8] P. Żenczykowski, *Acta Phys. Pol. B* **33** 1833 (2002).
[9] M. Gronau, J.L. Rosner, *Phys. Rev.* **D58**, 113005 (1998).
[10] K. Anikeev *at al.*, `hep-ph/0201071`.
[11] Z. Luo, J.L Rosner, *Phys. Rev.* **D65**, 054027 (2002).
[12] J.L Rosner, in *Flavor Physics for the Millennium*, Boulder 2000, p.431, `hep-ph/0011355`.
[13] K.M. Watson, *Phys. Rev.* **88**, 1163 (1952).
[14] R. Seber , *Phys. Rev. Lett.* **13**, 32 (1964).
[15] V. Barger, R.J.N. Phillips, *Nucl. Phys.* **B32**, 93 (1971).
[16] B. Aubcrt, *et al.*, *Phys. Rev.* **D66**, 054024 (2002).
[17] The BaBar Collaboration, `hep-ph/0207065`.
[18] S. Chen *et al.*, [CLEO Collaboration], *Phys. Rev. Lett.* **85**, 525 (2000).
[19] M. Gronau, J.L Rosner, *Phys. Rev.* **D65**, 093012 (2002).
[20] Z.z. Xing, *Phys. Lett.* **B493**, 301 (2000).
[21] C.K. Chua, W.S. Hou, K.C. Yang, `hep-ph/0210002`.